Coordination Chemistry of *N*,*N*′-Bis(diphenylphosphanylmethyl)-2,3-dihydro-1*H*-perimidine – Lewis Acid-Base Complexes with the d^{10}-Metals Nickel(0) and Gold(I)

Sven Krieck, Daniel Schulze, Helmar Görls, and Matthias Westerhausen

Institute of Inorganic and Analytical Chemistry, Friedrich Schiller University Jena, Humboldtstrasse 8, D-07743 Jena, Germany

Reprint requests to Prof. Dr. Matthias Westerhausen. Fax: +49 3641 948132.
E-mail: m.we@uni-jena.de

Z. Naturforsch. **2014**, *69b*, 1299 – 1305 / DOI: 10.5560/ZNB.2014-4150
Received July 11, 2014

Dedicated to Professor Hubert Schmidbaur on the occasion of his 80th birthday

The addition reactions of *N*,*N*′-bis(diphenylphosphanylmethyl)-2,3-dihydro-1*H*-perimidine (**1**) with [$(cod)_2$Ni] and [(Ph_3P)AuCl] yield yellow [(**1**)Ni(η^4-cod)] (**2**) and colorless [(**1**)(Ph_3P)AuCl]·3MeOH (**3**), respectively. In these transition metal complexes of nickel(0) and gold(I) **1** acts as a bidentate chelating ligand. Crystal structures of [(**1**)Ni(η^4-cod)]·3THF (**2a**) and of cosolvent-free [(**1**)Ni(η^4-cod)] (**2**) reveal a distorted tetrahedral environment of the nickel atom. The gold(I) atom in **3** exhibits a very long Au–Cl bond of 296.2(1) pm. In contrast to the nickel complexes, compound **3** shows strong agostic interactions between gold(I) and a methylene fragment.

Key words: Nickel, Gold, Perimidine, Phosphane Oxides, Phosphanes, Agostic Interactions

Introduction

Bidentate phosphane ligands of the type Ph_2P–X–PPh_2 with organic linkers X play an important role in coordination chemistry and catalysis for the stabilization of low oxidation states and catalytic cycles (for reviews on recent developments on phosphane bases see [1 – 9]). Many of these derivatives are commercially available and represent commonly used bidentate Lewis bases; prominent representatives include chelate bases with X being CH_2 (dppm), $(CH_2)_2$ (dppe), $(CH_2)_3$ (dppp), and ferrocene-1,1′-diyl (dppf). These ligands offer plenty of possibilities of variations in order to tune electronic and steric properties and, hence, offer a rich coordination chemistry. Substituents at the phenyl groups and at the X backbone as well as the rigidity of X strongly influence the coordination behavior.

Therefore it is not surprising that these ligands of the general type Ph_2P–X–PPh_2 play key roles in the coordination chemistry of nickel(0) and gold(I) complexes. Numerous nickel(0) and gold(I)complexes of these bis-phosphanes are known containing bridging or bidentate ligands. Easily accessible *N*,*N*′-bis(diphenylphosphanylmethyl)-2,3-dihydro-1*H*-perimidine (**1**) [10] represents a bidentate diphosphane with a preorientation of the phosphane bases easing bidentate coordination behavior. Reactions of this bis-phosphane **1** with Rh(Cl)$(PPh_3)_3$ and Ir(Cl)(CO)$(PPh_3)_2$ generate a carbene leading to the formation of a pincer complex with metal-carbon bonds stabilized by coordination to the phosphane bases [10]. We were interested in the coordination behavior of **1** toward important catalytically active transition metals and therefore, medium hard nickel(0) and soft gold(I) fragments were chosen. Whereas nickel-mediated catalysis has been well-known for many years [11], gold-based reactions gained much interest only quite recently (for a selection of recent reviews see refs. [12 – 19]).

Results and Discussion

In order to study the coordination behavior of bis-phosphane **1**, $Ni(cod)_2$ (cod = cycloocta-1,5-diene) was suspended in THF, and *N*,*N*′-bis(diphenylphosphanylmethyl)-2,3-dihydro-1*H*-perimidine (**1**)

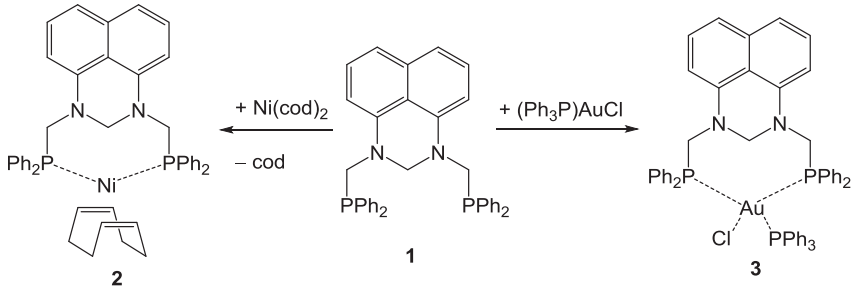

(1)

was added (Eq. 1). The reaction mixture was stirred for three days at ambient temperature. After partial removal of the solvent, yellow crystals of the nickel complex [(**1**)Ni(η^4-cod)]·thf (**2a**) precipitated at ambient temperature within two weeks. Recrystallization from toluene finally yielded pure [(**1**)Ni(η^4-cod)] (**2b**). The $^{31}P\{^1H\}$ NMR spectrum of **2** showed a low-field-shifted singlet at $\delta = +33.3$ ppm in comparison to free bis-phosphane **1** ($\delta = -26.5$ ppm). Even though this complex decomposes slowly in air at ambient conditions, it is much less sensitive in comparison to the starting material [Ni(cod)$_2$].

In order to study the coordination behavior of *N*,*N*′-bis(diphenylphosphanylmethyl)-2,3-dihydro-1*H*-perimidine (**1**) toward a very soft cation, this bis-phosphane and [(Ph_3P)AuCl] were combined in a Schlenk flask and dissolved in methanol (Eq. 1). After one week, the yellow solution was diluted with pentane and stored at –30°C. Colorless crystals of the addition product [(**1**)(Ph_3P)AuCl]·3MeOH (**3**) precipitated. In the $^{31}P\{^1H\}$ NMR spectrum two resonances at $\delta = +30.1$ and $+24.0$ ppm were observed for the PPh_3 ligand and coordinated **1**, respectively. Again, a significant low-field shift of the ^{31}P NMR resonance of **1** was detected. In the ^1H NMR spectrum the resonance of the N–CH_2–N fragment of the perimidine backbone ($\delta = 1.34$ ppm) exhibits a remarkable high-field shift. In free **1** a chemical shift of $\delta = 4.21$ ppm was observed for these hydrogen atoms.

The molecular structure of **2b** is depicted in Fig. 1; the molecular structure of **2a** is very similar, however, the quality of the structure analysis is slightly reduced due to large voids containing disordered solvent molecules. Selected structural parameters of **1**, **2a**, **2b**, and **3** are listed in Table 1. The P–C_{aryl} bonds to the phenyl groups are significantly shorter than the P–C_{alkyl} distances to the methylene moieties. The P1–Ni1–P2 bond angles of 108.4(1)° (**2a**) and 108.5(1)° (**2b**) are close to an ideal tetrahedral angle as expected for an sp^3 hybridized d^{10} metal atom. The structural parameters of complexes with the (η^4-cod)Ni fragment and phosphane ligands are compared in Table 2. The values of **2a** and **2b** lie in the expected regions with the Ni–P distances at the lower end. The P–Ni–P bond angle of the bidentate phosphane **1** is comparable to the value of [(cod)Ni(PPh_3)$_2$] [5] supporting the lack of steric strain.

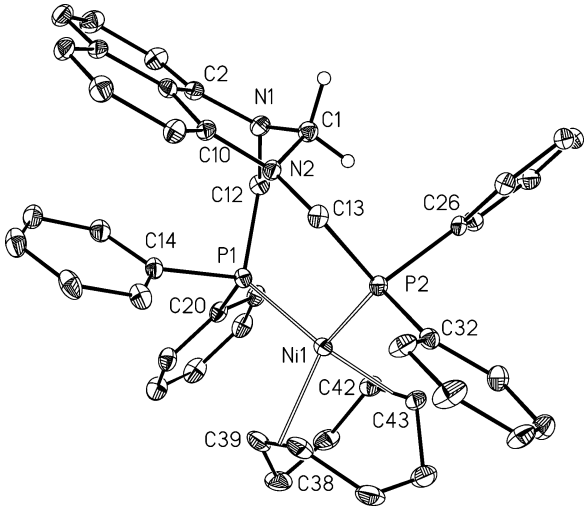

Fig. 1. Molecular structure and atom numbering scheme of **2b**. The ellipsoids represent a probability of 30 %. H atoms are omitted for clarity reasons with the exception of those at C1 which are shown with arbitrary radii.

The molecular structure of the gold(I) complex **3** is shown in Fig. 2. The striking structural feature is the elongated Au–Cl bond. In starting [(Ph_3P)AuCl] with dicoordinate gold(I) an Au–Cl distance of 229.03(4) pm is observed [25], whereas in **3** with a tetracoordinate gold(I) center an elongation of 67 pm for the Au1–Cl1 bond is found. The Au1–P distances vary in the very narrow range from 236.8(1) to 238.6(1) pm

Table 1. Comparison of the structural parameters of the *N*,*N*′-bis(diphenylphosphanylmethyl)-2,3-dihydro-1*H*-perimidine ligand (**1**) with those of the complexes **2a**, **2b**, and **3**.

	1	**2a**	**2b**	**3**
N1–C1	146.2(2)	143.0(5)	143.5(4)	144.4(3)
N2–C1	145.3(2)	144.8(5)	146.3(4)	144.9(4)
N1–C2	139.9(2)	142.5(5)	141.9(4)	138.2(4)
N1–C12	145.4(2)	145.9(5)	145.7(4)	144.2(4)
N2–C10	143.4(2)	140.4(5)	140.2(4)	139.9(3)
N2–C13	147.6(2)	143.9(5)	144.6(4)	145.2(3)
Σ(C–N1–C)	350.3	347.7	348.2	359.2
Σ(C–N2–C)	335.7	352.7	352.2	353.6
N1–C1–N2	111.7(1)	112.0(4)	111.3(3)	109.4(2)
N1–C12–P1	111.04(10)	118.5(3)	118.6(2)	108.4(2)
N2–C13–P2	110.14(9)	112.5(3)	112.5(2)	110.3(2)
P1–C12	186.4(2)	190.6(4)	190.5(4)	185.5(3)
P1–C14	183.1(2)	182.8(4)	184.6(3)	181.1(3)
P1–C20	183.5(2)	184.3(4)	183.9(3)	181.6(3)
P2–C13	186.2(2)	187.2(5)	186.9(3)	186.5(3)
P2–C26	183.6(2)	184.1(5)	186.3(3)	182.0(3)
P2–C32	183.9(2)	184.7(5)	184.9(3)	182.6(3)
Σ(C–P1–C)	302.4	297.9	299.6	310.8
Σ(C–P2–C)	300.7	301.3	298.4	311.3
P1–L[a]	–	217.2(1)	218.5(1)	238.6(1)
P2–L[a]	–	214.7(1)	2152(1)	236.8(1)

[a] Distance between phosphorus and Lewis acid L.

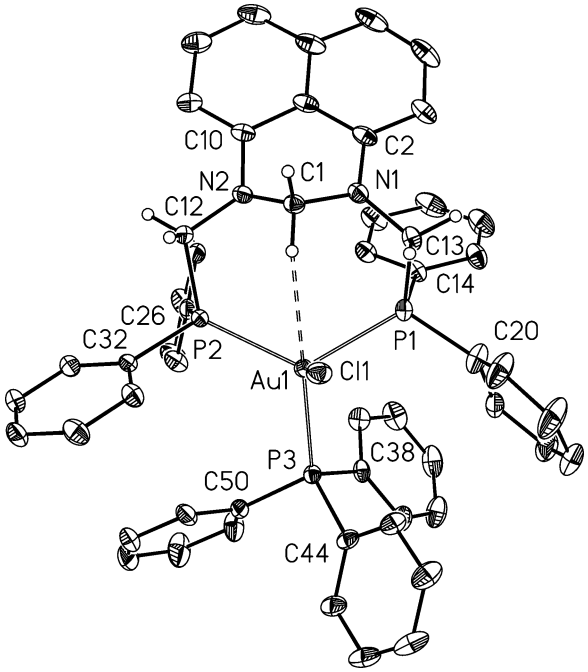

Fig. 2. Molecular structure and atom numbering scheme of **3**. The ellipsoids represent a probability of 30 %. H atoms are neglected for clarity reasons with the exception of those of the methylene moieties which are drawn with arbitrary radii. The broken bond symbolizes the agostic interaction between Au1 and C1-bound H1B.

and are elongated compared to that in [(Ph_3P)AuCl] (Au–P 223.13(4) pm [25]) due to the larger coordination number. The P1–Au1–P2 bond angle of 124.2 (1)° of the fragment [(**1**)Au] is significantly larger than that observed for the nickel complex **2**. The sum of the angles Σ(P–Au–P) of 355.3° (only considering the P–Au–P angles and neglecting the chloride coordination) supports the interpretation of a distorted trigonal-planar coordination of gold(I) by three phosphane ligands. A covalent interpretation could assume a sp^2 hybridized d^{10} metal atom with the chloride ion binding to the remaining p_z orbital. This interpretation is in agreement with the severe elongation of the Au1–Cl1 bond compared to that of [(Ph_3P)AuCl] with the Cl atom bound to an sp hybrid orbital of a gold(I) atom in a linear coordination sphere.

Table 2. Comparison of selected structural parameters [bond lengths (average values in pm) and angles (deg)] of (cod)Ni complexes with phosphane ligands.

Compound	Ni–C	Ni–P	P–Ni–P	P–C_{aryl}	P–C_{alkyl}	Ref.
[(cod)Ni(**1**)]·3THF (**2a**)	210.8	215.9	108.4(1)	184.0	188.9	this work
[(cod)Ni(**1**)] (**2b**)	210.6	216.8	108.5(1)	184.9	188.7	this work
[(cod)Ni(PPh_3)$_2$]	200.7[a]	218.6	107.6(1)	183.9	–	[20]
[(cod)Ni(PPh_2Et)$_2$]	211.2	218.7	108.2	183.8	185.4	[21]
[(cod)Ni{binaph(PPh_2)$_2$}]	211.0	217.4	97.4(1)	183.7	–	[22]
[(cod)Ni{(Ph_2P)$_2$NLi(thf)$_3$}]	208.6	219.6	69.4(1)	184.6	168.9[b]	[23]
[(cod)Ni{(Ph_2P)$_2$NSnMe_3}]	209.5	217.0	73.2(1)	183.9	172.0[b]	[23]
	209.3	215.6	73.2(1)	183.2	170.7[b]	
[(cod)Ni{(Ph_2P-C_5H_4)$_2$Co}]	212.6	219.0	106.3(2)	183.7	–	[24]

[a] Distance between nickel and the midpoint of the C=C double bond;
[b] average P–N bond lengths.

Table 3. Coordination spheres of the gold(I) atoms in complexes containing tetracoordinate metal atoms with one chloride and three phosphane ligands (bond lengths in pm, angles in deg).

Complex	Au–Cl	Au–P1	Au–P2	Au–P3	Σ(P–Au–P)	Ref.
[(**1**)(Ph_3P)AuCl]·3MeOH (**3**)	296.2(1)	238.6(1)	236.8(1)	237.3(1)	355.3	
[(Ph_3P)$_3$AuCl]	271.0(2)	239.5(2)	240.4(2)	243.1(2)	352.3	[26]
[(dppp)(Ph_3P)AuCl]	292.8(2)	239.0(2)	238.6(2)	230.5(2)	356.1	[27]
[($C_{12}H_8PPh$)$_3$AuCl]	273.5(2)	235.9(1)	238.2(1)	237.4(2)	341.7	[28]
[(dppf)$_{1.5}$AuCl]$_2$	292.9(3)	234.5(3)	239.1(3)	240.5(3)	354.8	[29]
[{$C_4H_2N_2(PPh_2)_2$}$_{1.5}$AuCl]	270.3(1)	236.83(6)	236.8(1)	236.8(1)	341.3	[30]
[{$CH_2(P(OCH_2CF_3)_2)_2$}$_{1.5}$AuCl]	277.1(1)	235.1(1)	235.6(1)	237.7(1)	355.1	[31]
[($Ph_2PC{\equiv}CPPh_2$)$_3$(AuCl)$_2$]	264.0(1)	234.2(1)	237.2(1)	240.7(1)	339.1	[32]
	263.8(1)	234.1(1)	236.6(1)	236.6(1)	343.2	
[{($Ph_2PC_6H_4$)$_2$PPh}AuCl]	251.2(1)	246.1(1)	232.1(1)	236.9(1)	293.5	[33]
[(Ph_2P–X–PPh_2)(Ph_3P)AuCl] [a]	277.8(1)	236.0 (1)	243.5(1)	234.3(1)	348.6	[34]
[($ROCH_2PPh_2$)$_3$(AuCl)$_2$] [b]	301.2(6)	237.1(6)	237.9(6)	238.4(6)	359.9	[35]

[a] *rac*-[1-(Diphenylphosphino)-2,1′-{1-(diphenylphosphino)butane-1,3-diyl}ferrocene]-chloro-(triphenylphosphane)-gold(I) toluene solvate; [b] *catena*-[{μ-5,11,17,23-tetrakis(*tert*-butyl)-25,26,27,28-tetrakis(diphenylphosphinomethoxy)calix(4)arene-*P*,*P*′,*P*″-dichloro-digold(I) dihydrate].

In Table 3 the coordination environments of tetracoordinate gold(I) atoms in complexes with one chloro and three phosphane ligands are compared. Remarkably, the Au–Cl distances vary within a large range from approx. 251 to 301 pm with complex **3** being at the high end of this region. The smallest value was observed for [{($Ph_2PC_6H_4$)$_2$PPh}AuCl] with a tridentate ligand with a rather small bite allowing only a small sum of the angles Σ(P–Au–P) of 293.5° [33]. Despite the variation of the Au–Cl distances, the Au–P bond lengths lie in a rather narrow range.

Another remarkable feature is the agostic bonding in the gold(I) complex **3**. In Fig. 2, this bonding is shown with a dashed line between Au1 and the C1-bound hydrogen atom $H1B_{C1}$ (Au1···H1B 294 pm). The corresponding Au1···C1 distance of 359.3 pm is significantly smaller than the corresponding value in the nickel complex **2b** (N1–$H1_{C1}$ 345 pm, Ni1···C1 397.3 pm) despite the fact that Ni(0) has a smaller radius than Au(I) as evidenced by the metal-phosphorus bond lengths (av. Ni–P 216.8 pm, Au–P 237.7 pm). Two kinds of interactions between metal atoms and C–H bonds can be distinguished [36] (for reviews on agostic interactions see *e. g.* [37–41]). On the one hand, agostic bonds consist of a side-on-bound C–H bond to a metal atom and can be considered as a closed 3-center-2-electron bond with small M–H–C angles and rather short M···H and M···C contacts. On the other hand, anagostic interactions are of largely electrostatic nature and can be described by an open 3-center-2-electron bond with large M–H–C angles and rather large M···H and M···C distances. In the gold(I) complex an Au1···H1B–C1 bond angle of 124.7° hints toward an agostic interaction.

Conclusion

The *N*-bound diphenylphosphanylmethyl side arms of *N*,*N*′-bis(diphenylphosphanylmethyl)-2,3-dihydro-1*H*-perimidine (**1**) introduce steric strain leading to significantly different sums of the angles at the nitrogen atoms. Coordination of Lewis acids and formation of tetracoordinate phosphorus atoms lead to a significant low-field shift of the $^{31}P\{^1H\}$ resonances with the largest value of $\delta = 33.3$ ppm for the nickel complex **2**. In comparison to the other derivatives, the gold(I) complex **3** shows a remarkable high-field shift ($\delta(^1H) = 1.34$ ppm) for the methylene protons of the perimidine unit. This finding hints toward a close contact between the heavy noble metal and the protons (agostic interaction). These attractive interactions between Au1 and C1 in complex **3** enforce a significantly widened P1–Au1–P2 bond angle of 124.2(1)°. In addition, this attraction between the gold(I) atom and the N1–CH_2–N2 moiety leads to an acute N1–C1–N2 bond angle and to rather small N–C–P angles. In the nickel complex **2**, there are repulsive forces between this fragment and the metal atom as evidenced by an acute P1–Ni1–P2 angle of 108.4(1)°. In addition, a large N1–C1–N2 bond angle of 112.0(4)° and widened N–C–P angles are observed.

The influence of Lewis acids on the structural parameters of **1** is rather small. Coordination of nickel(0) and gold(I) leads to the formation of an eight-membered ring. In these metallacycles the coordination sphere of the nitrogen atoms is flattened (the sums of the angles Σ(C–N–C) are enlarged), and in the gold(I) derivative **3** an almost trigonal-planar environment is observed. The pyramidalization of the phosphane bases is much less influenced by the binding of Lewis acids.

N,*N*′-Bis(diphenylphosphanylmethyl)-2,3-dihydro-1*H*-perimidine (**1**) is available by a simple straightforward procedure and therefore resembles an attractive bidentate ligand for transition metals. The low-oxidized nickel(0) and gold(I) fragments are stabilized and exhibit only a moderate sensitivity toward moisture and air at ambient conditions. The nickel(0) complexes **2** are significantly more durable under ambient conditions than [$(cod)_2$Ni] and could offer an alternative as a precatalyst in nickel-mediated catalysis.

Experimental

General comments

All manipulations were carried out under an inert argon or nitrogen atmosphere using standard Schlenk techniques. The solvents were dried according to standard procedures. Deuterated THF and benzene were dried over sodium, degassed, and saturated with argon. The yields given are not optimized. ^{1}H and ^{13}C{^{1}H} NMR spectra were recorded on Bruker AC 200, AC 400 or AC 600 spectrometers. Chemical shifts are reported in parts per million (ppm) relative to Me_4Si (^{1}H, ^{13}C) or relative to phosphoric acid (^{31}P) as external standards. The residual signals of [D_8]THF or [D_6]benzene were used as internal standards. Starting bisphosphane **1** was prepared according to a literature protocol [10].

*Synthesis of (η^4-cycloocta-1,5-diene)-{N,N′-bis(diphenylphosphanylmethyl)-2,3-dihydro-1H-perimidine}-nickel(0) (**2**)*

To a suspension of 432 mg of $(cod)_2$Ni (1.57 mmol) in 4 mL of THF, a solution of 890 mg of *N*,*N*′-bis(diphenylphosphanylmethyl)-2,3-dihydro-1*H*-perimidine (**1**) (1.57 mmol) in 8 mL of THF was slowly added. The reaction mixture was stirred for 3 d. Then the volume of the solution was reduced, and storage at 4°C yielded 0.284 g of yellow crystalline **2**$(THF)_3$ (0.30 mmol, 19%). Decomp.: >109°C. – ^{1}H NMR (400 MHz, [D_6]benzene, 297 K): $\delta = 2.20$ (m, CH_2(COD)), 3.78 (dd, 2H, NCH_2N), 4.40 (dd, 4H, PCH_2), 5.57 (m, CH(COD)), 6.43 (dd, 2H, naph-CH), 6.77 – 7.55 (multiplets, arom. CH). – ^{13}C{^{1}H} NMR (100.6 MHz, [D_6]benzene, 297 K): $\delta = 25.7$ (s, CH_2, THF), 28.3 (br, NCH_2N), 29.5 (s, CH_2, COD), 67.8 (s, CH_2O, THF), 108.1 (CH, naph), 119.1 (s, CH, naph), 126.1 (s, CH, naph), 127.1 (d, CH, C_6H_5, $J = 8$ Hz), 128.8 (s, CH, COD), 128.7 (s, C, C_6H_5), 132.5 (d, CH, C_6H_5, $J = 12$ Hz), 133.7 (d, C, C_6H_5,$J = 12$ Hz), 135.7 (s, C, naph), 145.3 (s, C, naph). – ^{31}P{^{1}H} NMR (162 MHz, [D_6]benzene, 297 K): $\delta = 33.27$ (s). – EI-MS: m/z(%) = 566 (4) [ligand]$^+$, 381 (12) [M–PPh_2]$^+$, 183 (94) [M–PPh_2–CH_2PPh_2]$^+$. – ESI-MS: m/z(%) = 621 (100) [M–COD]$^+$. – IR: (cm^{-1}): $\nu = 498$ s, 635 m, 673 m, 393 vs, 736 m, 744 m, 815 m, 858 w, 1012 w, 1065 m, 1136 w, 1207 w, 1228 w, 1409 m, 1433 m, 1589 s, 2855 w, 3050 w. – Elemental analysis of **2**$(THF)_3$: $C_{57}H_{64}N_2NiO_3P_2$ (945.77), theor. (found): C 72.39 (73.46); H 6.82 (7.04); N 2.96 (3.22) %.

*Synthesis of chloro-{N,N′-bis(diphenylphosphanylmethyl)-2,3-dihydro-1H-perimidine}-(triphenylphosphane)-gold(I) (**3**)*

N,*N*′-Bis(diphenylphosphanylmethyl)-2,3-dihydro-1*H*-perimidine (**1**) (248 mg, 0.44 mmol) and [(Ph_3P)AuCl] (206 mg, 0.42 mmol) were combined in a Schlenk flask, and at r. t. 8 mL of methanol was added. The reaction mixture was stirred for one week. To the yellow solution a few milliliters of pentane were added. At –30°C, 114 mg of colorless crystals of **3**$(MeOH)_3$ (0.13 mmol, 30%) precipitated. M.p. 193°C. – ^{1}H NMR (400 MHz, $CDCl_3$, 297 K): $\delta = 1.34$ (s, 2H, NCH_2N), 3.45 (s, CH_3(MeOH)), 4.66 (d, 4H, PCH_2), 6.37 (d, 2H, naph-CH), 6.86 – 7.36 (multiplets, arom. CH). – ^{13}C{^{1}H} NMR (100.6 MHz, $CDCl_3$, 297 K): $\delta = 49.8$ (d, PCH_2, $J = 9$ Hz), 50.7 (s, CH_3OH), 67.7 (br, NCH_2N), 104.3 (s, CH, naph), 117.0 (s, C, naph), 125.9 (s, CH, naph), 128.0 (s, C, C_6H_5), 129.7 (d, C_6H_5, $J = 16$ Hz), 132.2 (br, C_6H_5), 133.7 (d, C, C_6H_5, $J = 14$ Hz), 135.4 (s, C, naph), 142.8 (s, C, naph). – ^{31}P{^{1}H} NMR (162 MHz, $CDCl_3$, 297 K): $\delta = 23.95$ (s), 30.09 (s, broad). – EI-MS: m/z(%) = 566 (22) [ligand]$^+$, 381 (54) [M–PPh_2]$^+$, 183 (100) [M–PPh_2–CH_2PPh_2]$^+$. – ESI-MS: m/z(%) = 763 (100) [M–Cl–PPh_3]$^+$. – IR: (cm^{-1}): $\nu = 490$ s, 521 s, 617 m, 665 m, 690 s, 741 s, 804 m, 833 m, 586 w, 997 w, 1026 m, 1040m, 1095 m, 1141 m, 1253 m, 1418 m, 1433 m, 1480 m, 1592 s, 2817 m, 3051 m. – Elemental analysis of **3**$(MeOH)_3$: $C_{40}H_{44}AuClN_2O_3P_2$ (895.16), theor. (found): C 53,67 (54.70); H 4.95 (5.02); N 3.13 (2.46) %.

Crystal structure determinations

The intensity data were collected on a Nonius KappaCCD diffractometer using graphite-monochromated MoK_α radiation. Data were corrected for Lorentz and polarization effects

Table 4. Crystal structure data of compounds **1**–**3**.

Compound	**1**	**2a**	**2b**	**3**
Emperical formula	$C_{37}H_{32}N_2P_2$	$C_{45}H_{44}N_2NiP_2 \cdot C_4H_8O$ + disordered solvent	$C_{45}H_{44}N_2NiP_2$	$[C_{55}H_{47}AuN_2P_3]Cl \cdot$ 3MeOH
M_r, g mol^{-1}	566.59	805.58[a]	733.47	1157.40
T, °C	–140(2)	−140(2)	−140(2)	−140(2)
Crystal system	monoclinic	trigonal	monoclinic	orthorhombic
Space group	$P2_1/n$	$R\bar{3}$	$P2_1/n$	$Pbcn$
a, Å	10.1906(2)	29.1323(4)	9.6451(2)	36.7106(5)
b, Å	17.6780(3)	29.1323(4)	19.0788(3)	12.6674(2)
c, Å	16.0615(2)	29.0914(4)	19.6178(3)	22.3284(3)
α, deg	90	90	90	90
β, deg	90.128(1)	90	95.633(1)	90
γ, deg	90	120	90	90
V, Å^3	2893.46(8)	21381.8(5)	3592.57(11)	10383.3(3)
Z	4	18	4	8
$\rho_{calcd.}$, g cm^{-3}	1.30	1.13[a]	1.36	1.48
μ, cm^{-1}	1.8	5.1[a]	6.7	30.2
Measured data	17 226	10 199	24 400	64 320
Unique data/R_{int}	6574/0.027	10 199/0.060	8238/0.082	11 870/0.028
Data with $I > 2\,\sigma(I)$	5758	7027	6014	10 661
$R1$ $[I > 2\,\sigma(I)]$[b]	0.0388	0.0754	0.0623	0.0287
$wR2$ (all data, on F^2)[c]	0.0934	0.2650	0.1139	0.0624
S[d]	1.064	1.114	1.160	1.094
Res. dens., e Å^{-3}	0.32/−0.30	2.26/−1.05	0.40/−0.43	0.80/−0.90
CCDC	974493	974495	1013051	974496

[a] These derived parameters do not include the contribution of the disordered solvent; [b] $R1 = \Sigma||F_o| - |F_c||/\Sigma|F_o|$; [c] $wR2 = [\Sigma w(F_o^2 - F_c^2)^2/\Sigma w(F_o^2)^2]^{1/2}$, $w = [\sigma^2(F_o^2) + (AP)^2 + BP]^{-1}$, where $P = (\mathrm{Max}(F_o^2, 0) + 2F_c^2)/3$; [d] $S = \mathrm{GoF} = [\Sigma w(F_o^2 - F_c^2)^2/(n_{obs} - n_{param})]^{1/2}$.

but not for absorption [42, 43]. The structures were solved by Direct Methods (SHELXS [44]) and refined by full-matrix least-squares techniques against F_o^2 (SHELXL-97 [44]). The crystal structure of **2a** contains large voids, filled with disordered solvent molecules. Their contribution to the structure factors was secured by back-Fourier transformation using the routine SQUEEZE as incorporated in the program PLATON [45].

All hydrogen atoms of **1** and **2b** were located by difference Fourier syntheses and refined isotropically. All other hydrogen atoms were included at calculated positions with fixed isotropic parameters. All non-disordered, non-hydrogen atoms were refined anisotropically [44]. Crystallographic data as well as structure solution and refinement details are summarized in Table 4. XP (Siemens Analytical X-ray Instruments, Inc.) was used for structure representations [46].

CCDC 974493 (**1**), 974495 (**2a**), 1013051 (**2b**), and 974496 (**3**) contain the supplementary crystallographic data for this paper. These data can be obtained free of charge from The Cambridge Crystallographic Data Centre *via* www.ccdc.cam.ac.uk/data_request/cif.

Acknowledgement

This work was supported by the Verband der Chemischen Industrie (VCI/FCI, Frankfurt/Main, Germany). Infrastructure of our institute was partly provided by the EU (European Regional Development Fund, EFRE).

[1] A. R. Popescu, F. Teixidor, C. Vinas, *Coord. Chem. Rev.* **2014**, *269*, 54 – 84.
[2] C. D. Swor, D. R. Tyler, *Coord. Chem. Rev.* **2011**, *255*, 2860 – 2881.
[3] D. J. M. Snelders, G. van Koten, R. J. M. Klein Gebbink, *Chem. Eur. J.* **2011**, *17*, 42 – 57.
[4] G. Bouhadir, A. Amgoune, D. Bourissou, *Adv. Organomet. Chem.* **2010**, *58*, 1 – 107.
[5] M. L. Clarke, J. J. R. Frew, *Organomet. Chem.* **2009**, *35*, 19 – 46.
[6] D. S. Glueck, *Chem. Eur. J.* **2008**, *14*, 7108 – 7117.
[7] Z. Freixa, P. W. N. M. van Leeuwen, *Coord. Chem. Rev.* **2008**, *252*, 1755 – 1786.

[8] F. Mohr, S. H. Priver, S. K. Bhargava, M. A. Bennett, *Coord. Chem. Rev.* **2006**, *250*, 1851 – 1888.
[9] L.-C. Liang, *Coord. Chem. Rev.* **2006**, *250*, 1152 – 1177.
[10] A. F. Hill, C. M. A. McQueen, *Organometallics* **2012**, *31*, 8051 – 8054.
[11] See *e. g.*: B. Cornils, W. A. Herrmann, *Applied Homogeneous Catalysis with Organometallic Compounds: A Comprehensive Handbook*, Wiley-VCH, Weinheim, **2000**.
[12] R. E. M. Brooner, R. A. Widenhoefer, *Angew. Chem. Int. Ed.* **2013**, *52*, 11714 – 11724.
[13] F. Barabe, P. Levesque, B. Sow, G. Bellavance, G. Betournay, L. Barriault, *Pure Appl. Chem.* **2013**, *85*, 1161 – 1173.
[14] A. S. K. Hashmi, *Top. Organomet. Chem.* **2013**, *44*, 143 – 164.
[15] L. T. Ball, G. C. Lloyd-Jones, C. A. Russell, *Science* **2012**, *337*, 1644 – 1648.
[16] M. Rudolph, A. S. K. Hashmi, *Chem. Soc. Rev.* **2012**, *41*, 2448 – 2462.
[17] M. Peixoto de Almeida, S. A. C. Carabineiro, *ChemCatChem* **2012**, *4*, 18 – 29.
[18] A. S. Dudnik, N. Chernyak, V. Gevorgyan, *Aldrichim. Acta* **2010**, *43*, 37 – 46.
[19] A. S. K. Hashmi, M. Bührle, *Aldrichim. Acta* **2010**, *43*, 27 – 33.
[20] H. Maciejewski, A. Sydor, B. Marciniec, M. Kubicki, P. B. Hitchcock, *Inorg. Chim. Acta* **2006**, *359*, 2989 – 2997.
[21] R. Kempe, J. Sieler, D. Walther, *Z. Kristallogr.* **1996**, *211*, 565 – 566.
[22] D. J. Spielvogel, W. M. Davis, S. L. Buchwald, *Organometallics* **2002**, *21*, 3833 – 3836.
[23] M. Said, D. L. Hughes, M. Bochmann, *Polyhedron* **2006**, *25*, 843 – 852.
[24] N. Liu, X. Li, X. Xu, Z. Wang, H. Sun, *Dalton Trans.* **2011**, *40*, 6886 – 6892.
[25] A. O. Borrissova, A. A. Korlyukov, M. Y. Antipin, K. A. Lyssenko, *J. Phys. Chem. A* **2008**, *112*, 11519 – 11522.
[26] P. G. Jones, G. M. Sheldrick, J. A. Muir, M. M. Muir, L. B. Pulgar, *J. Chem. Soc., Dalton Trans.* **1982**, 2123 – 2125.
[27] F. Caruso, M. Rossi, J. Tanski, C. Pettinari, F. Marchetti, *J. Med. Chem.* **2003**, *46*, 1737 – 1742.
[28] S. Attar, W. H. Bearden, N. W. Alcock, E. C. Alyea, J. H. Nelson, *Inorg. Chem.* **1990**, *29*, 425 – 433.
[29] A. Houlton, D. M. P. Mingos, D. M. Murphy, D. J. Williams, *Acta Crystallogr.* **1995**, *C51*, 30 – 32.
[30] V. J. Catalano, M. A. Malwitz, S. J. Horner, J. Vasquez, *Inorg. Chem.* **2003**, *42*, 2141 – 2148.
[31] J. L. Dempsey, A. J. Esswein, D. R. Manke, J. Rosenthal, J. D. Soper, D. G. Nocera, *Inorg. Chem.* **2005**, *44*, 6879 – 6892.
[32] M. Bardají, M. T. de la Cruz, P. G. Jones, A. Laguna, J. Martínez, M. D. Villacampa, *Inorg. Chim. Acta* **2005**, *358*, 1365 – 1372.
[33] J. Zank, A. Schier, H. Schmidbaur, *J. Chem. Soc., Dalton Trans.* **1999**, 415 – 420.
[34] G. Lübbe, R. Fröhlich, G. Kehr, G. Erker, *Inorg. Chim. Acta* **2011**, *369*, 223 – 230.
[35] G. B. Dieleman, D. Matt, A. Harriman, *Eur. J. Inorg. Chem.* **2000**, 831 – 834.
[36] M. Brookhart, M. H. Green, G. Parkin, *Proc. Natl. Acad. Sci. (USA)* **2007**, *104*, 6908 – 6914.
[37] J. Saßmannshausen, *Dalton Trans.* **2012**, *41*, 1919 – 1923.
[38] J. C. Green, M. L. H. Green, G. Parkin, *Chem. Commun.* **2012**, *48*, 11481 – 11503.
[39] O. Kühl, *Chem. Soc. Rev.* **2011**, *40*, 1235 – 1246.
[40] M. Lein, *Coord. Chem. Rev.* **2009**, *253*, 625 – 634.
[41] E. Clot, O. Eisenstein, *Struct. Bonding* **2004**, *113*, 1 – 36.
[42] R. Hooft, COLLECT, Nonius Kappa CCD Data Collection Software, Nonius BV, Delft (The Netherlands) **1998**.
[43] Z. Otwinowski, W. Minor in *Methods in Enzymology*, Vol. 276, *Macromolecular Crystallography*, Part A (Eds.: C. W. Carter Jr, R. M. Sweet), Academic Press, New York, **1997**, pp. 307 – 326.
[44] G. M. Sheldrick, *Acta Crystallogr.* **2008**, *A64*, 112 – 122.
[45] A. L. Spek, *Acta Crystallogr.* **2009**, *D65*, 148 – 155.
[46] XP, Siemens Analytical X-ray Instruments Inc., Karlsruhe (Germany) **1990**; Siemens Analytical X-ray Instruments Inc., Madison, Wisconsin (USA) **1994**.